Structural, elastic, optoelectronic and magnetic properties of CdHo$_2$S$_4$ spinel: a first-principle study

I HATRAF[1], O MERABIHA[1], T SEDDIK[1,*], H BALTACHE[1], R KHENATA[1], R AHMED[2], SALEEM A KHAN[3], A BOUHEMADOU[4], SIKANDER AZAM[3] and S BIN OMRAN[5]

[1]Laboratoire de Physique Quantique de la Matière et de la Modélisation Mathématique (LPQ3M), Université de Mascara, 29000 Mascara, Algeria

[2]Department of Physics, Faculty of Science, Universiti Teknologi Malaysia, UTM, 81310 Skudai, Johor, Malaysia

[3]New Technologies - Research Center, University of West Bohemia, Univerzitni 8, 306 14 Pilsen, Czech Republic

[4]Laboratory for Developing New Materials and their Characterization, Department of Physics, Faculty of Science, University of Setif 1, 19000 Sétif, Algeria

[5]Department of Physics and Astronomy, College of Science, King Saud University, P.O. Box 2455, Riyadh 11451, Saudi Arabia

*Author for correspondence (sedik_t@yahoo.fr)

Abstract. We report the results of the full-potential linearized augmented plane wave (FP-LAPW) calculations on the structural, elastic, optoelectronic and magnetic properties of CdHo$_2$S$_4$ spinel. Both the generalized gradient approximation (GGA) and Trans-Blaha modified Becke-Johnson potential (TB-mBJ) are used to model the exchange-correlation effects. The computed lattice parameter, internal coordinate and bulk modulus are in good agreement with the existing experimental data. According to the calculated elastic moduli, CdHo$_2$S$_4$ is mechanically stable with a ductile nature and a noticeable elastic anisotropy. The ferromagnetic phase of CdHo$_2$S$_4$ is energetically favourable compared to non-magnetic one, with a high magnetic moment of about 8.15 μ_B. The calculated band structure demonstrates that the title compound is a direct band gap semiconductor. The TB-mBJ yields a band gap of ∼1.86 and ∼2.17 eV for the minority and majority spins, respectively. The calculated optical spectra reveal a strong response in the energy range between the visible light and the extreme UV regions.

Keywords. CdHo$_2$S$_4$; spinel rare earth; TB-mBJ; electronic band structure; magnetic properties; optical properties.

1. Introduction

In recent times, ternary compounds with chemical formula CdRE$_2$X$_4$ (RE = rare earth, X = S, Se) called rare earth chalcogenides spinel have created a lot of interest in researchers because of their interesting optoelectronic and magnetic properties [1–10]. This family of compounds had been prepared and recognized for the first time by Suchow and Stemple [11]. In some studies on electronic properties [12,13], these spinels were reported as insulating materials with band gap values that are equal and greater to 2 eV, highlighting their potential for device applications like LED, photoconductors, photoelectrochemical solar cells and photocatalysis [14,15].

Among this family, the CdHo$_2$S$_4$ compound is characterized firstly by Fujii *et al* [16] and they postulate an intermediate spinel structure which means that just 60% of Cd^{2+} is occupying a tetrahedral site and the other 40% are empty and unoccupied by Ho^{+3}. Conversely, using an X-ray powder pattern, the CdHo$_2$S$_4$ is reported to crystallize in normal spinel structure [13] when Cd^{2+} occupy the tetrahedral sites and Ho^{+3}, the octahedral sites. Then, Dor *et al*

[17] studied structural and magnetic properties of CdHo$_2$S$_4$ and pointed out its spinel structure besides observing its ferromagnetic nature in the ground state. On the other hand, through electron microscopy and X-ray diffraction, Bakker *et al* [18] also confirmed the normal spinel structure for CdHo$_2$S$_4$. Moreover, they also observed a transition from this structure to rocksalt structure at high temperature. Schevciw *et al* [19] measured the optical absorption edge and suggest an optical band gap of 2.32 eV for the CdHo$_2$S$_4$ compound. Very recently, CdHo$_2$S$_4$ chalcogenide spinel has been experimentally prepared through a two-step route, has shown the signature of magnetic ordering at transition temperature T_c ≈ 0.87 K [20]. Although, some experimental studies on CdHo$_2$S$_4$ compound are found in the literature, a comprehensive theoretical study is rarely reported for this material. In view of this, the aim of the present study is to predict theoretically structural, optoelectronic, elastic and magnetic properties of CdHo$_2$S$_4$ spinel to provide reference data for further experimentations to uncover its potential for technological applications and further to complete existing information on this compound.
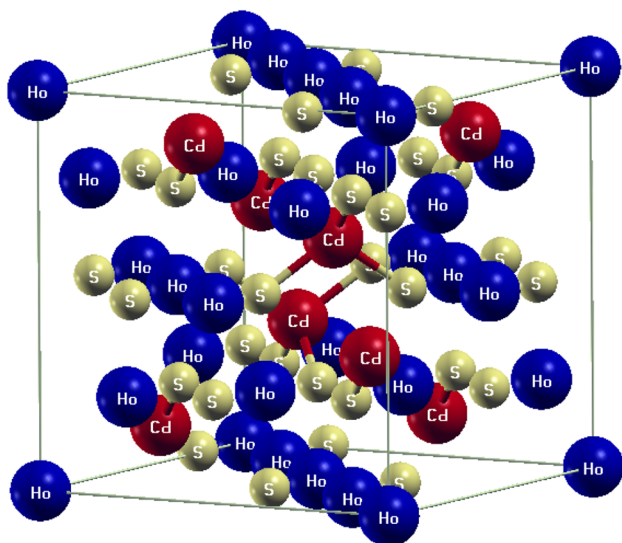
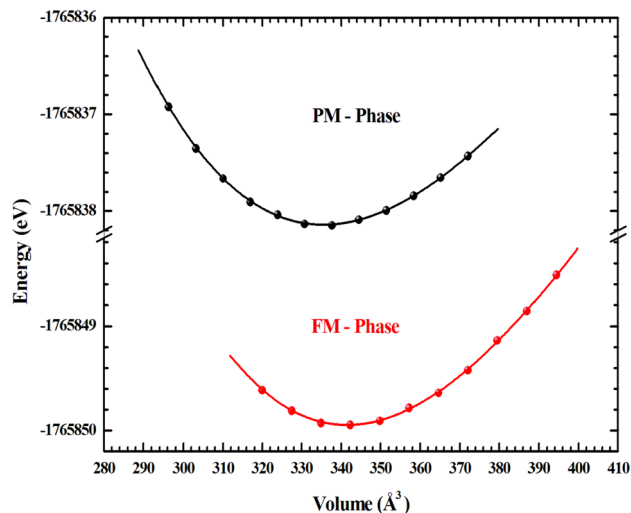**Figure 1.** Crystal structure of CdHo$_2$S$_4$.

Figure 2. Calculated total energy as a function of the primitive cell volume for CdHo$_2$S$_4$ in both non-magnetic (PM) and ferromagnetic (FM) phases.

2. Method of calculation

All calculations were performed using the full-potential linearized augmented plane wave (FP-LAPW) method as implemented in the WIEN2k code [21]. Both the generalized gradient approximation (GGA-PBE) [22] and Trans-Blaha modified Becke-Johnson potential (TB-mBJ) [23,24] methods were used to treat the exchange-correlation effects. The radii of the MT spheres for Cd, Ho and S atoms were 2.36, 2.50 and 2.09 atomic units (a.u.), respectively. A set of 56 k-points were used to perform a reliable integration over the Brillouin zone (BZ). A cutoff parameter $R_{MT}K_{max} = 7$, where R_{MT} is the smallest muffin-tin sphere and K_{max} is the largest reciprocal lattice vector, was used in the plane wave expansion. These values were obtained by ensuring total energy convergence.

3. Results and discussion

3.1 *Structural properties*

CdHo$_2$S$_4$ is crystallized in a closely packed FCC crystal structure, space group Fd-3m (n. 227). The unit cell of CdHo$_2$S$_4$ contains 8 Cd atoms positioned at (3/8, 3/8, 3/8), 16 Ho atoms at (0, 0, 0) and 32 S atoms at (u, u, u) with $u = 0.2456$ (figure 1).

Hence, the crystalline structure of CdHo$_2$S$_4$ is characterized by two free parameters; the internal coordinate u and the lattice parameter a. The optimized value of u is achieved by relaxing the S atoms in the unit cell. Variations of the total energy (E) *vs.* primitive cell (V) for both the non-magnetic (PM) and ferromagnetic (FM) phases of CdHo$_2$S$_4$ are presented in figure 2.

Table 1. Calculated equilibrium unit cell volume (V_0), lattice parameter (a_0), bulk modulus (B) and its pressure derivative B', and the optimized internal coordinate u for the ferromagnetic (FM) and non-magnetic (PM) phases of the CdHo$_2$S$_4$.

Phase		V_0	A_0	B	B'	u
PM	Present	1341.914	11.029	68.287	4.216	0.2425
FM	Present	1364.678	11.092	72.864	4.888	0.2425
	Expt. [17]		11.167			0.2456
	[02]	1389.30	11.158			

The obtained $E(V)$ data were fitted to the Murnaghan's [25] equation of state (EOS) to obtain the ground state properties of the title compound, such as the lattice parameter a_0, the bulk modulus B_0 and its pressure derivative B'. The obtained results are summarized along with the available experimental data in table 1. The calculated lattice parameter a_0 is in excellent agreement with the experimental data [2,17]; and the relative deviation is <0.7%.

3.2 *Elastic properties*

The elastic constants (C_{ij}) of CdHo$_2$S$_4$ are calculated using the variation of the total energy *vs.* strain approach [26]. The calculated three independent elastic constants for the cubic CdHo$_2$S$_4$ are $C_{11} = 134.76$ GPa, $C_{12} = 29.48$ GPa and $C_{44} = 23.41$ GPa. To the best of our knowledge, this is the first prediction of the elastic constants for CdHo$_2$S$_4$. The obtained elastic constants satisfy the generalized elastic stability criteria for a cubic crystal [27]:

$$(C_{11} - C_{12}) > 0, (C_{11} + 2C_{12}) > 0, C_{11} > 0, C_{44} > 0.$$
$$(1)$$

Table 2. Calculated bulk modulus (B, in GPa), shear modulus (G, in GPa), Young's modulus (E, in GPa), Poison's ratio (ν, dimensionless), anisotropy factor (A) and universal elastic anisotropy factor (A^U).

$B_V = B_R$	B_H	G_V	G_R	G_H
64.57	64.57	35.10	30.09	32.59
B_H/G_H	E	ν	A	A^U
1.98	83.70	0.28	0.44	0.83

Table 3. Calculated total magnetic moment (M_{Total}, in the μ_B units), contributions of each atom (M_{Cd}, M_{Ho} and M_S, in the μ_B units) and contribution of the interstitial region ($M_{Int.}$ in the μ_B units) for CdHo$_2$S$_4$.

	M_{Total}	M_{Cd}	M_{Ho}	M_S	$M_{Int.}$
Present	8.155	0.007	3.827	0.045	0.310
Expt.	10.3[a], 10.6[a]				
	10.6[b], 10.7[c]				

[a]Ref. [17]; [b]ref. [19]; [c]ref. [19].

This indicates that CdHo$_2$S$_4$ is mechanically stable. The C_{44} is much lower than the C_{11}, indicating that the resistance to the unidirectional compression is larger than the resistance to the pure shear deformation in this compound.

From the estimated elastic constant C_{ij}, one can determine other polycrystalline elastic moduli, such as the bulk modulus B, shear modulus G, Young's modulus E and Poisson's ratio ν through the Voigt–Reuss–Hill approximation [28–30]. According to Voigt and Reuss approximation, the bulk modulus B and shear modulus G for a polycrystalline compound of a cubic system are given by the following expressions:

$$B_V = B_R = B_H = \frac{(C_{11} + 2C_{12})}{3}, \tag{2}$$

$$G_V = \frac{(C_{11} - C_{12} + 3C_{44})}{5}, \tag{3}$$

$$G_R = \frac{5(C_{11} - C_{12})C_{44}}{[4C_{44} + 3(C_{11} - 3C_{12})]}, \tag{4}$$

$$G_H = (G_V + G_R)/2. \tag{5}$$

Subsequently, the Young's modulus E and Poison's ratio ν can be calculated using the following formulae:

$$E = 9B_H G_H/(3B_H + G_H), \tag{6}$$

$$\nu = (3B_H + E)/6B_H. \tag{7}$$

The obtained results using the above equations for the mentioned polycrystalline elastic moduli are shown in table 2. Poison's ratio ν can provide information on the bonding nature of a material. The ν value of 0.28 indicates an ionic contribution in the intraatomic bonding in CdHo$_2$S$_4$. Pugh [31] has proposed a simple empirical relationship that correlates the elastic moduli of material with their plastic properties. If the B/G ratio is >1.75, then the material is ductile; otherwise, it is brittle. The predicted B/G ratio for CdHo$_2$S$_4$ is 1.98, proving that this compound is ductile. A ductile material is resistant to thermal shocks.

To evaluate the degree of elastic anisotropy in CdHo$_2$S$_4$, we calculated the anisotropic factor A defined as follows:

$$A = \frac{2C_{44}}{(C_{11} - C_{12})}. \tag{8}$$

For an isotropic crystal, A should be equal to one and any divergence from the unity indicates the extent of the elastic anisotropy. Our computed value of the anisotropic factor A indicates a very large elastic anisotropy of CdHo$_2$S$_4$. The universal index A^U [32] defined as follows:

$$A^U = \frac{5G_V}{G_R} + \frac{B_V}{B_R} - 6. \tag{9}$$

This was also used to evaluate the elastic anisotropy of the title compound. For isotropic crystals, A^U is equal to zero, whereas the deviation of A^U from zero defines the extent of the elastic anisotropy. Our estimated value of A^U is higher than zero, indicating that CdHo$_2$S$_4$ is characterized by a certain elastic anisotropy.

3.3 *Magnetic properties and stability*

Variations of the total energy *vs.* primitive cell for the FM and PM phases of CdHo$_2$S$_4$ are presented in figure 2, which demontrates that the FM phase is more stable than the PM phase, which is in a good agreement with the experiments [2,17]. The calculated magnetic moments are shown in table 3 when compared to the experimental data [2,17,20].

Our results illustrate clearly that the total magnetic moment of CdHo$_2$S$_4$ is principally a contribution of the holmium ions with a small contribution from the Cd and S atoms. To some extent, poor harmony between calculated and experimental values may be ascribed to the used exchange-correlation functional, which is inappropriate to handle the $5f$ electrons in CdHo$_2$S$_4$.

3.4 *Electronic properties*

The calculated band structures for spin-up and spin-down channels using both the GGA-PBE and TB-mBJ for CdHo$_2$S$_4$ are shown in figure 3a and b. The zero energy is set to the top of the valence band. It is found that CdHo$_2$S$_4$ is a direct band gap semiconductor ($\Gamma - \Gamma$) for both the majority and minority spin channels.
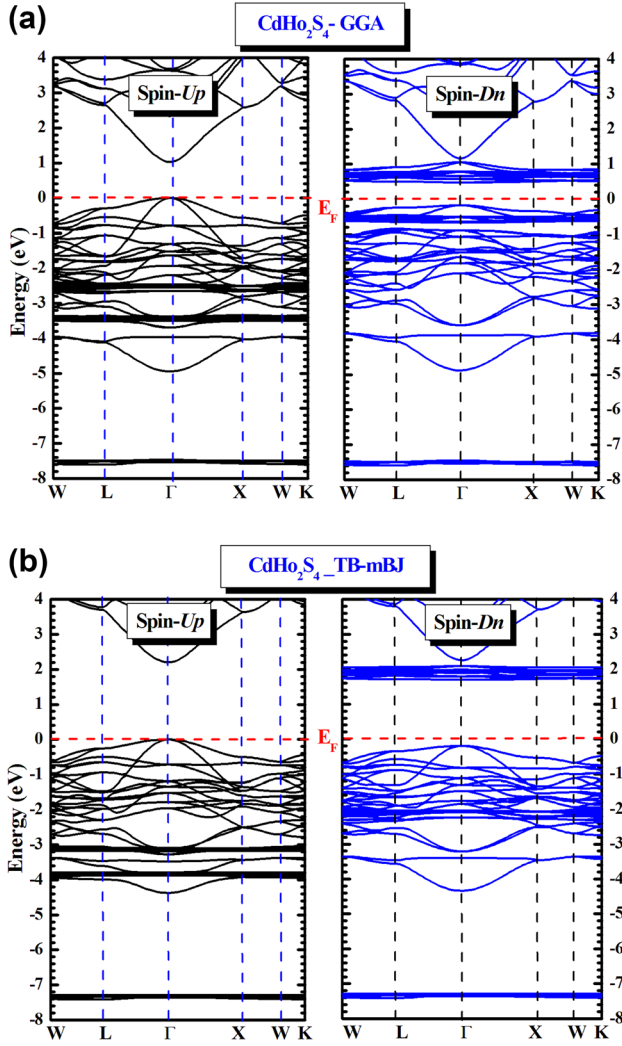
(a)

(b)

Figure 3. Calculated spin-polarized band structure of CdHo$_2$S$_4$ within the (**a**) GGA and (**b**) TB-mBJ functionals.

Table 4 shows that the calculated band gap values using the TB-mBJ are much larger than those obtained using the PBE-GGA for both channels. The calculated band gaps using the TB-mBJ, which are 1.86 and 2.17 eV for the majority and minority spins, respectively, agree reasonably with the measured ones (2.32 eV) [19].

Figure 4 presents the calculated total and partial densities of states (TDOS and PDOS) using the TB-mBJ for both channels, i.e., minority and majority spins.

From figure 4, one can observe that the TDOS is divided into three regions in the case of majority spin, and in four regions for minority spin. The first sharp peak, located at around −7.5 eV, in the TDOS spectra of both spin channels arises mainly from the filled Cd 'd' states with a small contribution of the S 'p' states. The upper valence band (UVB) group is separated from the first sharp peak by a gap of about 3.6 eV in the minority spin and 3.4 eV in the majority spin. In the majority spin, the second region of the UVB, lying between the top of the valence band and down to ∼4.3 eV below the Fermi level (E_F), shows mainly two different intense peaks. The first peak around −3.9 eV consists principally of the Ho 'f' states and the second one at about −3.2 eV is dominated by the mixed Ho 'f' states and S 'p' states. On the other hand, there is one main peak in the minority spin in the region of −2.1 eV contributed by the Ho 'f, d' states and S 'p' states. The region above E_F around 2 eV in the minority spin is fundamentally dominated by the Ho 'f' states and the region in the energy range from 4 eV to the high energy in the conduction band is mainly dominated by the mixture of the Ho 'd' and Cd 'p' states for both the spin channels. We identified the occurrence of an overlap between the Ho 'f, d' and S 'p' states in the valence band, indicating a significant degree of hybridization between these states, which suggests a covalent character of the Ho–S bond.

3.5 *Optical properties*

The calculated real $\varepsilon_1(\omega)$ and imaginary $\varepsilon_2(\omega)$ parts of the dielectric function $\varepsilon(\omega)$ of CdHo$_2$S$_4$ for an incident photon energy ($\hbar\omega$) in the 0–45 eV range are depicted in figure 5a. The $\varepsilon_2(\omega)$ spectrum shows three sharp peaks located at 2.8, 4.8 and 7.5 eV. These peaks are mainly generated by the direct transition from the S '$3p$' states to the Ho '$4f$' states and from the Cd '$4p$' states to the Ho '$4f$' states. Beyond this energy range, $\varepsilon_2(\omega)$ curve drops off rapidly with increasing photon energy. With further increase in the photon energy almost from 10 to 25 eV, a minimum absorption is noted, however, another peak at about 28.2 eV is found in the absorption spectrum. The zero frequency limit of $\varepsilon_1(\omega)(\varepsilon_1(0))$ is an important optical quantity used to determine the dielectric response of a material to the static electric field. It is found that $\varepsilon_1(0)$ is equal to 5.15 in CdHo$_2$S$_4$. The spectrum of $\varepsilon_1(\omega)$ shows an appreciable peak in the ultraviolet (UV) region, at about 4.31 eV, followed by another high peak at about 6.9 eV. The spectrum of $\varepsilon_1(\omega)$ further illustrates a steep decrease until it

Table 4. Comparison of calculated direct band gaps values for CdHo$_2$S$_4$ using both GGA and TB-mBJ. The used unit is eV.

	L – L		Γ – Γ		X – X		W – W	
	Up	Dn	Up	Dn	Up	Dn	Up	Dn
GGA	2.894	0.750	1.11	0.65	3.123	0.842	3.904	0.955
TB-mBJ	3.947	2.066	2.17	1.86	4.067	2.263	4.775	2.425
Expt. [19]				2.32				
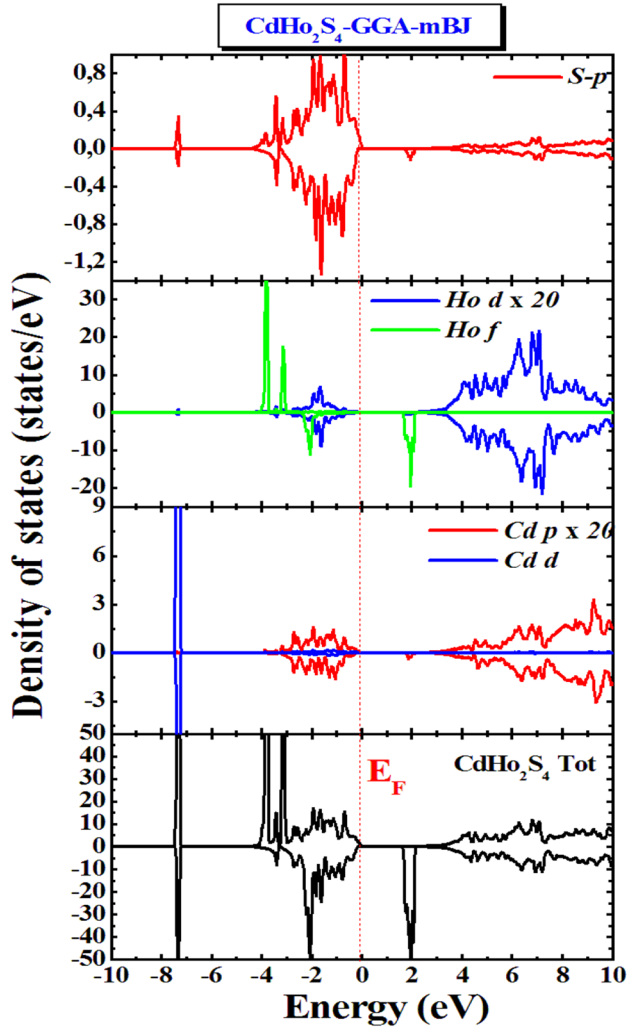
Figure 4. Total and partial projected densities of states (TDOS and PDOS) of CdHo$_2$S$_4$ using TB-mBJ potential.

Figure 5. Calculated optic spectra using the TB-mBJ potential.

becomes negative in the energy range where the phonon is damped, and then slowly increases towards zero.

The calculated reflectivity coefficient $R(\omega)$, refractive index $n(\omega)$ and absorption coefficient $\alpha(\omega)$ are shown in figure 5. At zero energy, the reflectivity $R(\omega)$ (figure 5b) is ∼15% and then increases with some oscillations in the energy range from 2 to 17 eV. In addition, the $R(\omega)$ approaches to the maximum value of 35.6% in the UV region in coincidence with the minimum value of the real part of the $\varepsilon_1(\omega)$ and then, the reflectivity $R(\omega)$ shows a sharp drop in the energy around 18.9 eV, which corresponds to the so-called screened plasma frequency ω_P. At the energy of ∼29.1 eV, CdHo$_2$S$_4$ exhibits a reflectance of ∼14.1% and approaches zero at high photon energy.

Figure 5c visualizes the refractive index $n(\omega)$ spectra of CdHo$_2$S$_4$. The static refractive index $n(0)$ is equal to ∼2.27. The $n(\omega)$ spectrum increases from the static value to small peaks in the visible light region and reaches a maximum of
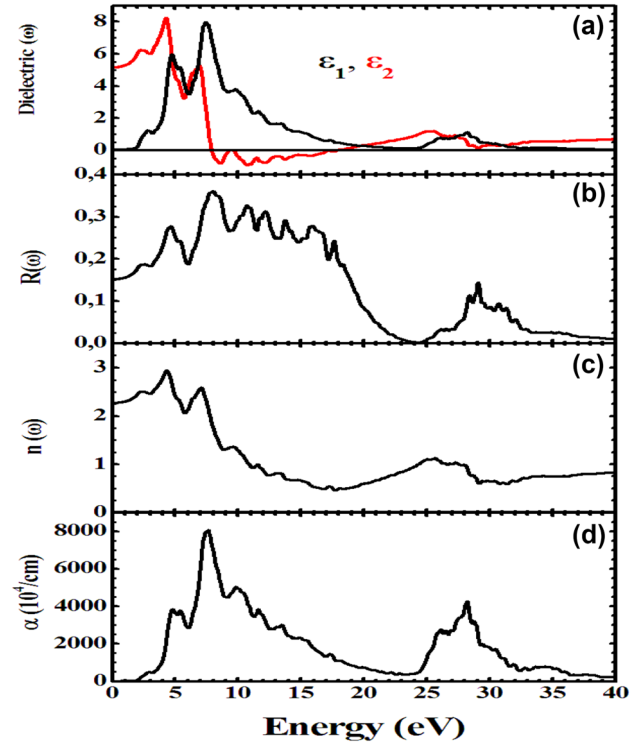
2.95 in the UV region, and then decreases rapidly with increasing photon energy to its minimum value, which is smaller than one in the UV region.

The absorption coefficient is an important parameter that measures the absorption of the electromagnetic wave energy, while traversing the unit thickness of a material [33]; it depends on the wavelength of electromagnetic wave and the material as well. Figure 5d shows the plotted absorption coefficient spectrum of CdHo$_2$S$_4$. A wide range of absorption region, from visible light to UV with a maximum at 7.6 eV, is observed. Furthermore, at high energy, CdHo$_2$S$_4$ exhibits a strong absorption in the energy range from 25 to 32 eV. Accordingly, these results indicate that CdHo$_2$S$_4$ can absorb all the frequencies between the visible light and extreme UV regions.

4. Conclusions

Detailed calculations were performed using the FP-LAPW approach within the PBE-GGA and TB-mBJ to investigate the structural, elastic, magnetic and optoelectronic properties of the CdHo$_2$S$_4$ spinel. Calculated ground state properties are in good agreement with the available experimental data. The title compound shows a ductile nature and a noticeable elastic anisotropy. The FM phase of CdHo$_2$S$_4$ is energetically favourable with a high magnetic moment. The CdHo$_2$S$_4$ is

a direct band gap semiconductor. Using TB-mBJ, the predicted direct band gap (Γ–Γ) value is $\sim$1.86 and $\sim$2.17 eV for the majority and minority spins, respectively, which are in good agreement with the experiments. Our calculated optical spectra over a photon energy ranging from 0 to 45 eV, identified that the $CdHo_2S_4$ spinel expresses a strong response in the energy range between the visible light and extreme UV regions.

Acknowledgements

References

[1] Pawlak L, Falkowski K and Pokrzywnicki S 1981 *J. Solid State Chem.* **37** 228
[2] Lau G C, Freitas R S, Ueland B G, Schiffer P and Cava R J 2005 *Phys. Rev. B* **72** 054411
[3] Lago J, Zivković I, Malkin B J, Rodriguez-Fernandez J, Ghigna P, Dalmas de Reotier P *et al* 2010 *Phys. Rev. Lett.* **104** 247203
[4] Flahaut J 1968 *Progress in the science and technology of the rare earths* (ed.) L Eyring (Oxford: Pergamon Press) Ch. 6 vol III p 209
[5] Flahaut J, Guittard M, Partie M, Pardo M P, Golabi S M and Domange L 1965 *Acta Cryst.* **19** 14
[6] Tomas A, Shilo I and Guittard M 1978 *Mater. Res. Bull.* **13** 857
[7] Tomas A, Guittard M, Flahaut J, Guymont M, Portier R and Gratias D 1986 *Acta Cryst.* **B42** 364
[8] Pokrzywnicki S and Czopnik A 1975 *Phys. Status Solidi B* **70** K85
[9] Pokrzywnicki S 1975 *Phys. Status Solidi B* **71** K111
[10] Partie M, Flahaut J and Domange L 1964 *Acad. Sci. Paris* **258** 2585
[11] Suchow L and Stemple N R 1963 *J. Electrochem. Soc.* **110** 187C; 1964 **111** 191
[12] Aliev O M, Agaev A B and Azadaliev R A 1997 *Inorg. Mater.* **33** 1123
[13] Yim W M, Fan A K and Stofko E J 1973 *J. Electrochem. Soc.* **120** 441
[14] W Zhang, H Yang, W Fu, M Li, Y Li and Yu W 2013 *J. Alloys Compd.* **561** 10
[15] Sawant S S Shinde, Bhosale C H and Rajpure K Y 2010 *Sol. Energy* **84** 1208
[16] Fujii H, Okamoto T and Kamigaichi T 1972 *J. Phys. Soc. Jpn.* **32** 1432
[17] BenDor L and Shilo J 1980 *Solid State Chem.* **35** 278
[18] Bakker M, Vollebregt F H A and Plug C M 1982 *J. Solid State Chem.* **42** 11
[19] Schevciw O and White W B 1983 *Mat. Res. Bull.* **18** 1059
[20] Yaouanc A, Dalmas de Réotier P, Bertin A, Marin C, Lhotel E, Amato A *et al* 2015 *Phys. Rev. B* **91** 104427
[21] Blaha P, Schwarz K, Madsen G K H, Kvasnicka D and Luitz J 2001 *WIEN2k, An augmented plane wave plus local orbitals program for calculating crystal properties* (Austria: Vienna University of Technology)
[22] Perdew J P, Burke K and Ernzerhof M 1996 *Phys. Rev. Lett.* **77** 3865
[23] Tran F and Blaha P 2009 *Phys. Rev. Lett.* **102** 226401
[24] Hosseini S M 2008 *Phys. Status Solidi B* **245** 2800
[25] Murnaghan F D 1944 *Proc. Natl. Acad. Sci. USA* **30** 244
[26] Mehl M J 1993 *Phys. Rev. B* **47** 2493
[27] Wang J and Yip S 1993 *Phys. Rev. Lett.* **71** 4182
[28] Hill R 1952 *Proc. Phys. Soc. Lond. A* **65** 34951
[29] Voigt 1928 *Lehrbuch der kristallphysik* (Teubner: Leipzig) vol 52
[30] Reuss A and Angew A 1929 *Math. Phys.* **9** 49
[31] Pugh S F 1954 *Philos. Mag.* **45** 823
[32] Ranganathan S I and Ostoja-Starzewski M 2008 *Phys. Rev. Lett.* **101** 55504
[33] Wooten F 1972 *Optical properties of solids* (New York: Academic Press)